Project Deliverable

Project Number:	Project Acronym:	Project Title:
325275	SAPPHIRE	System Automation of PEMFCs with Prognostics and Health management for Improved Reliability and Economy
Instrument: Collaborative Project (CP)		**Thematic Priority** FUEL CELL AND HYDROGEN JOINT UNDERTAKING

Title: **Analysis of Degradation Mechanisms**	
Contractual Delivery Date: January 31, 2014	**Actual Delivery Date:** February 10, 2014
Start date of project: May 1, 2013	**Duration:** 36 months
Organisation name of lead contractor for this deliverable: FESB, University of Split	**Document version:** Version 1.1
Organisation notes:	

Dissemination level (Project co-funded by the European Commission within the Seventh Framework Programme)		
PU	Public	**PU** Public
PP	Restricted to other programme participants (including the Commission)	
RE	Restricted to a group defined by the consortium (including the Commission)	
CO	Confidential, only for members of the consortium (including the Commission)	

Authors (organizations):

Dario Bezmalinovic, FESB, University of Split

Frano Barbir, FESB, University of Split

Abstract : PEM fuel cells degrade over time. The loss of cell potential is the most obvious symptom of degradation. Degradation may affect either one of the four major losses in fuel cells, namely activation polarization, ohmic losses, concentration polarization and hydrogen crossover losses. The report first addresses these symptoms, and then degradation mechanisms of different fuel cell components are discussed, namely catalyst and catalyst layer, membrane, and gas diffusion layer. For each of these some mitigation strategies are discussed. For each of degradation mechanism the key stressors are identified and standardized accelerated test protocols are presented. Experiments that were conducted at FESB with the goal of gaining practical experience and understanding of underlying degradation mechanisms. Two series of experiments were conducted with two of the most severe stressors, namely prolonged exposure to open circuit voltage, and potential cycling.

Revision History

Rev.	Date	Description	Author (Organisation)
1.0	Feb. 10, 2014	Draft submitted to project for comments	Frano Barbir (FESB)
1.1	Mar. 23, 2014	Corrected version submitted	Frano Barbir (FESB)

1. Degradation Symptoms

Performance of PEM fuel cells degrades over time. As performance of fuel cells is conveniently measured by their potential (actually potential vs. current density), the loss of potential is the most obvious symptom of their degradation. Generally, there are four major sources of performance losses, or polarizations, in fuel cells: 1) activation polarization (kinetic losses), 2) ohmic or resistive losses 3) concentration polarization or mass transport losses and 4) internal currents and/or crossover losses. It is relatively easy to determine from simple performance diagnostics which type of polarization has increased over period of time. By simply plotting the polarization-change over time curves one should be able to extract contribution of different polarizations changes on the cell's performance. The polarization-change curve is a curve obtained by subtracting the actual cell potential from the potential at the beginning of life (BOL) for a spectrum of current densities. Since the cell's performance normally degrades over the course of time, the polarization-change curve should always result in ever increasing positive voltage values. This, however, implies that the polarization curve taken at the BOL is defined as the peak performance and must be taken after the break-in period, in which the cell performance actually increases with the time. Needless to say, the operating conditions at which the polarization curves were taken at any point of time should be the same for all curves. Also, by measuring polarization curves before and after applying recovery procedures one should be able to distinguish recoverable from irrecoverable degradation. By further breaking down the polarization change-curve to the four curves each representing one of the aforementioned polarizations one should ideally get the curves as shown in Figure 1.
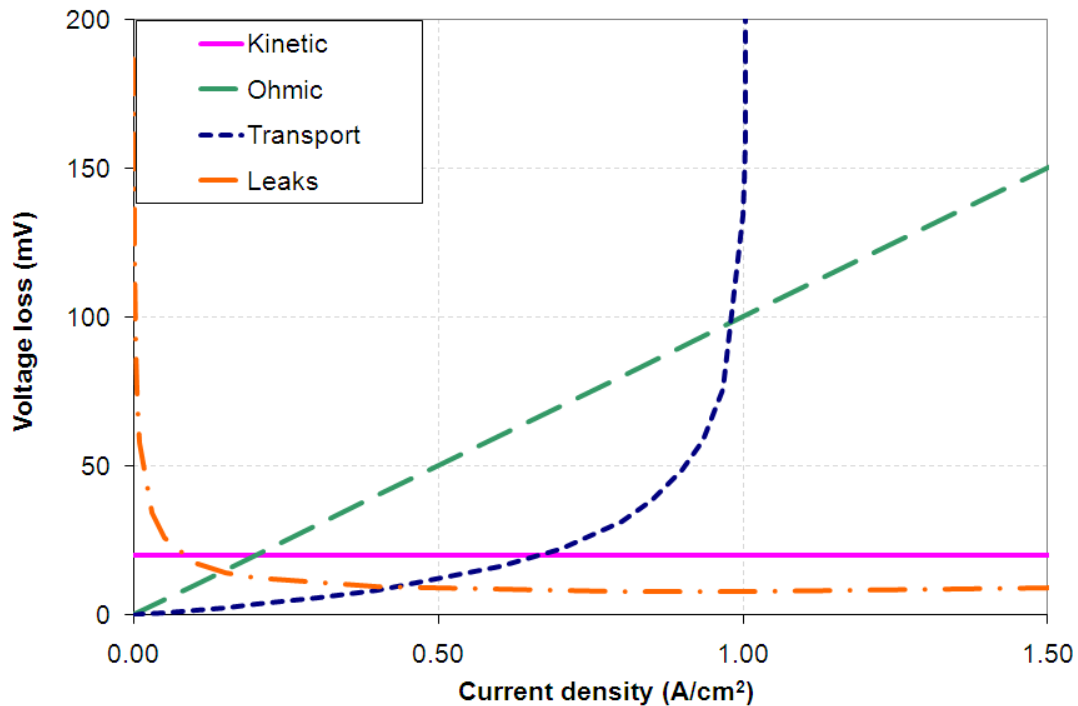
Figure 1 Limiting cases of polarization-change curves

The limiting cases depicted in Figure 1 are obtained using a simple model for each type of polarization. The most often cited simplified model of polarization curve is [1]:

$$E_{cell} = E_{th} - b \, log \left(\frac{i}{i_o} \right) - iR - \frac{RT}{2F} ln \left(\frac{i_L}{i_L - i} \right) \tag{1}$$

The first term on the right side represents theoretical cell voltage, the second term represents activation loss, and third term is ohmic loss while the last term represents concentration loss. As this is a simplified equation it is valid only for $i > i_0$.

The first limiting case depicted in Figure 1, straight horizontal line, results from an increase in activation polarization. This means that the cell's performance losses caused by the increased kinetic losses are independent of current density. Increased kinetic losses are usually associated with a decreased exchange current density or a decrease in catalytic surface area (which in turn again reduces the apparent exchange current density) while Tafel slope does not appear to change much with catalyst degradation [2]. Decreasing i_o while keeping b and i constant in the second term of equation (1) results in a curve vertical offset.

The second limiting case, a straight line that intercepts the origin of the plot comes from an increase in ohmic resistance. This is usually caused by the increased ionic resistance in the membrane and the catalyst layers (CLs) due to problem with hydration or by the increased contact resistance between layers due to delamination.

FB – Analysis of Degradation Mechanisms

The third limiting case, an exponential curve is associated with the increased transport losses or concentration polarization. Polarization concentration is associated with the reactants' "difficulty" to reach the point of electrochemical reaction. The limiting current density is a current density that equals the reactant's rate of diffusion from the channel to reaction site. Drawing currents above this point is impossible because that would mean that the reactants are being consumed at a rate faster than they are being supplied. Any decrease in the limiting current density would result in an additional loss in the form of an exponential curve that would approach infinity as the current approaches the new limiting current density, as can be calculated from the last term in equation (1). However, the term for the concentration losses in equation (1) is more suitable for smooth planar electrodes, which is not the case in PEM fuel cells. Due to porous surface nature of the catalyst layer, and numerous discrete reaction sites, concentration polarization in the PEM fuel cells usually does not exhibit limiting current behavior. However, during transients it is possible to reach limiting currents.

And finally, the fourth limiting case is observed when "parasitic" or "stray" current or hydrogen crossover occur within the cell. Although stray currents and hydrogen crossover are two completely different phenomena, their ultimate effect on fuel cell performance is the same. Either some hydrogen crosses the membrane without participating in the electrochemical reaction or some current (of electrons) that is generated by hydrogen oxidation reaction does not reach the external circuit. Current loss and hydrogen loss may be expressed in same units either as amperes or mol/s (connected by Faraday's Law). Some hydrogen crossover is unavoidable because of the polymer structure and its water content. Hydrogen permeation through wet perfluorosulfonic acid polymer is one order of magnitudes larger than through dry polymer. However, excess hydrogen crossover may occur as a result of some degradation mechanism (such as morphological changes in the polymer). The effect of stray currents or hydrogen crossover on fuel cell performance is practically negligible except at open circuit and at very small external current densities. Equation (1) does not account for any current or hydrogen crossover losses, but they can be easily accounted for by adding actual or equivalent current loss, $i_{\text{x-over}}$, to the external current density in the numerator of the activation polarization term:

$$b\,log\left(\frac{i+i_{x-over}}{i_o}\right) \tag{2}$$

To conclude, plotting the change in cell performance over time is an efficient method to monitor degradation evolution over time and enables one to see the contribution of different polarization phenomena in overall degradation.

2. Decay mechanisms of different fuel cell components

A PEM fuel cell consists of repeating components including membrane, anode and cathode catalyst layers (CLs), anode and cathode gas diffusion layers (GDLs), bipolar plates and seals. Each of these components is susceptible to various decay mechanisms that can be associated with different types of performance losses. The most common decay mechanisms for the different cell components and their influence on the performance are listed in Table 1 [3].

2.1. Catalyst layers

As already explained, performance loss that is nearly independent of current density indicates increased activation losses. This type of loss is the result of decreased catalytic activity and therefore can only take place in the CL, cathode's or anode's. Catalyst layers are thin layers (≈10 μm thick) of finely dispersed catalyst particles (usually platinum) on catalyst support (usually high surface area carbon) located between the membrane and the GDL. It is where electrochemical reactions actually take place.

A decrease in catalytic activity most often results from a loss of electrochemically active surface area (ECSA) caused by Pt catalyst degradation. Pt catalyst particle growth is a process in which finely dispersed particles of platinum on catalyst support tend to agglomerate over time resulting in a decreased effective surface (cm^2/mg) of the catalyst. Different mechanisms are proposed to explain the previous process (Ostwald ripening, Pt migration…) and there is still no agreement on which mechanism is predominantly responsible for the catalyst coarsening [4][5]. Nevertheless, research has shown that the rate of catalyst particle growth is dependent on temperature, relative humidity (RH) and voltage. It increases with the increase of any of those parameters. While the temperature and RH operating ranges do not change much in the running cell, voltage can change from ≈1 V at open circuit voltage (OCV) to <0.6 V at the maximum load. However, Pt surface oxidizes at higher potentials, and, while this somewhat hampers the kinetics of the electrode, at the same time the thin oxide layer at the catalyst surface gives the catalyst very good protection from degradation. It is believed that at low Pt potentials (≈0.6 V) Pt surface is oxide-free, whereas at higher potentials (≈0.9 V) Pt oxide coverage may be quite high. Between these potentials the Pt surface is always covered with a certain amount of oxide species. It has been shown that the voltage cycling causes higher catalyst degradation than the potentiostatic experiments at the similar potentials. The ECSA loss is higher with the wider potential span and higher potential sweep rates. The reasoning behind this is that it takes certain amount of time for the protective oxide layer to form on the Pt catalyst surface. Therefore, cycling the CL between low (oxide free) and high potentials, exposes bare Pt catalyst to high potentials for certain amount of time. It is obvious that in a fuel cell only the cathode CL can experience such conditions, as there is no oxygen on the anode side. The loss of ECSA due to platinum particle growth is usually highest in the early stages of the fuel cell life and decreases with

time, because smaller catalyst particles are more prone to agglomeration. The loss of ECSA by catalyst particle growth is an irreversible decay mechanism.

Another common, also irreversible, decay mechanism that can cause loss of ECSA is corrosion of the carbon support. Carbon is not thermodynamically stable under conditions encountered in a PEM fuel cell, as the reversible potential of carbon corrosion is only 0.207 V vs. RHE. Luckily, due to its slow kinetics, carbon corrosion is negligible at potentials < 1.1 V. However, some transient states in a fuel cell can cause the voltage in a cell to locally reach values > 1.5 V, where the carbon corrosion rate is tremendous. Two modes are believed to cause this: 1) startup and shutdown transitions and 2) fuel starvation. The first mode is known to create air-fuel front in the cathode flow fields, resulting in cathode local potentials of > 1.4 V near the outlet during startup, or inlet during shutdown (if the purge is done with the air). This is also known as "reverse-current" mechanism due to the fact that in areas of high potentials ionic current through the cell goes in the opposite direction. The second mode is associated with a cell (or a portion of a cell) receiving less hydrogen than required by the Faraday's law. It may be caused by uneven flow distribution in a stack or by a blockage due to liquid water. As a consequence, anode potential rises to > 1.2 V, where anode catalyst support starts to be consumed as a fuel (as well as water through electrolysis). The overall cell voltage becomes negative, which is a good indicator that fuel starvation is taking place. Unlike this, in the case of air-fuel front cell voltage is not necessarily abnormal, which makes *in-situ* detection very difficult.

A decrease in catalytic activity can also be caused by adsorption of contaminants, like CO and H_2S on the anode (especially in the case of working with reformates) and NH_3 ad SO_x on the cathode. The impact on performance may not be independent of current density. For example, CO poisoning of the anode catalyst can significantly reduce the limiting current density for hydrogen oxidation. Oxidation of the platinum in the cathode CL can also reduce activity. However, contamination is reversible in most of the cases. Raising the potential of anode or cathode is often sufficient remove absorbed species, while prolonged operation of the cell in the absence of contaminants has been shown to remove species that adsorb on the cathode. Platinum oxides can be stripped by lowering the cathode potential [3].

Another, albeit reversible, decay mechanism that can cause a reduction in the ECSA is drying out of the CL. The so-called three phase zone needed for the electrochemical reaction to take place needs presence of the ionomer in the CL. It is well known that the ionomer's conductivity improves with its water content. Drying out of the CL or portions of it not only increases ohmic losses, but also shifts the electrochemical reaction to the sites with better ionic access, thus lowering the ECSA [6].

Table 1. Summary of different types of performance losses and possible decay mechanisms

Type of performance loss	Some Possible Decay Mechanisms		
	Anode diffusion media or catalyst layer	**Membrane**	**Cathode** diffusion media or catalyst layer
Catalytic activity Performance loss nearly independent of current density	**Possible causes** - Loss of catalyst area by sintering or dissolution - Contamination by adsorption*		**Possible causes** - Loss of catalyst area by sintering or dissolution - Contamination by adsorption* - Pt oxide formation*
Ohmic (ionic or electronic) Performance loss proportional to current density	**Possible causes** - Dryout of ionomer* - Contamination by foreign cations* - Increased contact resistance, intra- or interlayer	**Possible causes** - Dryout of membrane* - Contamination by foreign cations*	**Possible causes** - Dryout of ionomer* - Contamination by foreign cations* - Increased contact resistance, intra- or interlayer
Reactant mass transfer Performance loss exponential with current density	**Possible causes** - Flooding of diffusion media or catalyst layer* - Reactant channel blockage* - Carbon oxidation		**Possible causes** - Flooding of diffusion media or catalyst layer* - Reactant channel blockage* - Carbon oxidation
Crossover or Internal Current** (electrical or reactant) Performance loss primarily at low current densities		**Possible causes** -Short circuit through or around membrane (or seal materials) -Reactant leakage due to membrane (or seal) failure	

*   Often substantially reversible.

**   Reactant leakage, or electrical shorts, can also occur through the seal materials in the cell, which may be simjilar to a leak through the membrane, although reactant leakage may be external (*i.e.*, go overboard from the cell).

Changes in the catalyst layer do not result exclusively in catalytic activity decrease. Transport and ohmic losses can also take place in the CL. The most common case of reversible transport loss in the CL is excessive accumulation of water due to transient abnormal operating conditions. However, once the cell reaches normal operating conditions the performance should fully recover. Much more serious are the losses caused by the structural changes within the CL, which are irreversible. Oxidation of the carbon catalyst support can cause a loss of porosity in some localized areas, diminishing gas transport rates. CL can also lose its hydrophobicity over time, making it prone to flooding. Also, catalyst particle dissolution and agglomeration can induce transport losses, as reactants may have to penetrate deeper into the degraded CL to reach the reaction site. Another consequence of carbon corrosion is that relative percentage of conductive material in the CL may decrease (and even gaps can develop between layers), which can result in an increased contact resistance between layers. Transport and ohmic losses within the CL can result in so-called "double Tafel slope" [7].

2.1.1. Mitigation strategies

A lot of mitigation strategies for CL degradation have been proposed [4], including new materials (catalyst, support and binders) and fabrication processes. Still, the operating conditions play a major role in CL degradation. High voltage and temperature are known accelerators of both platinum dissolution and carbon corrosion. Lower RH was found to retard ECSA loss. However, with PFSA-based membranes operation with low RH is not desirable. Potential cycling enhances ECSA loss, with degradation higher with the wider potential span and higher potential sweep rates.

Some general guidelines could include:

- Avoid or minimize exposure to high voltages. Possible use of resistors with voltage control during startups and shutdowns.
- Avoid sudden changes of load. Possible use of capacitors or batteries to smooth out changes in potential. Sudden jumps from low to high potentials are particularly detrimental (e.g. stopping the load suddenly). It was shown that the gradual, instead of sudden, potential rise can significantly reduce ECSA degradation [4].
- Minimize creation of air-fuel fronts. Purge with inert gas if possible. If not purge with high flows [8].
- Operate the cell at moderate temperatures. Trade-off.
- Higher anode stoichiometries. Possible recycling.
- Switching to dry air before shutting down to dry out membrane and ionomer in the CL to lower the losses on startup [9].

FB – Analysis of Degradation Mechanisms

2.2. Membrane

There are three root causes of membrane failure [10]: 1) chemical degradation, 2) mechanical degradation and 3) shorting.

Chemical degradation is caused by the attack of the membrane by radical species generated as byproducts, or side reactions of the fuel cell electrochemical reactions causing polymer decomposition. This phenomenon causes thinning of the membrane and thus increases reactant crossover. Crossover results in highly exothermic combustion between O_2 and H_2 on the Pt surface, which can lead to the creation of pinholes in the membrane and ultimately membrane failure. The aggressive species generally accepted to cause the chemical decomposition of the membrane are hydroxyl radical (HO·), hydroperoxyl radical (HOO·) and hydrogen peroxide (H_2O_2). The most dangerous, HO· is created by the direct interaction of crossover gases on Pt surface in CL as well as on the Pt deposits within the membrane. Pt band within the membrane stems from the dissolution of Pt in cathode CL and it was found to enhance membrane degradation [11][12]. One generally accepted mechanism of PFSA membrane decomposition begins with the abstraction of hydrogen from the end perfluorocarboxylic acid group by OH· resulting in HF and CO_2 emission [13]. The rate of fluoride loss is considered to be an excellent measure for the membrane chemical degradation and it can be conveniently monitored *in-situ* by quantifying the fluoride emission in the exhaust gases. The degree of the membrane chemical degradation is often expressed in terms of total membrane fluoride inventory loss. However, this can be a very unreliable diagnostic technique as the membranes that experience highly localized degradation can fail at very low inventory losses (≈1%) [14], versus membranes with uniform degradation that can sustain losses >50% before failure.

Mechanical degradation is caused by cyclic or fatigue stresses imposed on the membrane via humidity and thermal fluctuations in a constrained cell. Fuel cell membranes often experience fluctuations in humidity and temperature due to fluctuating power demand or frequent startup and shutdowns. The constrained membrane in an assembled fuel cell experiences in-plane tensions and compressions due to shrinkage under dry conditions and swelling under wet conditions, respectively. Experiments have shown that the humidity in the fuel cell may generate stresses as high as 2.3 MPa and dimensional change of 11% [15]. Additionally, exposing a membrane to subzero temperatures can be very harmful not only to the membrane but to the CL as well. Water volume changes due to freezing can cause membrane and electrode structural damages resulting in an increase of the contact resistance between membrane and the CL, decreased ionic conductivity, and increased gas permeability [16][17].

Shorting is caused by electronic current passing through the membrane caused by over-compression and topographical irregularities in the neighboring components. Shorting not only reduces cell's performance, but also leads to local heat generation in the vicinity of the short. This damages the membrane and increases reactants' crossover, which adds additional stress to the membrane that can lead to membrane failure. Excursion to high voltages can be particularly dangerous as they can lead to sudden membrane failure. For example, if in an operating stack one cell develops significantly higher ohmic resistance than

the rest of the cells, it will experience excessive voltage drop that ultimately can become negative with values lower than -1 V.

All of the above mentioned modes of membrane degradation are irreversible degradations that result in permanent structural changes within the membrane. The influence on the fuel cell performance is typically according to the fourth limiting case described in in the first section. However, very often it can take quite a long time before even the slightest influence on the cell's performance is noticed and by that time, it can already be too late. As explained before, in the case of highly localized membrane degradation, overall hydrogen crossover can seem fairly constant over time and the OCV would not be influenced much. Also, one has to take into account that not all of the OCV decrease comes from the membrane: catalyst degradation also decreases OCV.

Reversible membrane degradation typically includes increased membrane resistance due to problems with hydration. Ionic conductivity of the PFSA based membranes is a strong function of ionomer hydration, which is function of RH. Increase in ohmic resistance can point to problems in reactants' humidification, cell's temperature rise or problems with water management. For example, fuel cells often experience rise in ohmic resistance at higher current densities due to electro-osmotic drag overpowering back-diffusion drag, thus drying out the ionomer on the anode side [1]. Other reason for the increased membrane resistance is contamination by metal cations (such as Fe^{2+} and Cu^{2+}) originating from metal bipolar or end plates. Similar to catalyst contamination, ionic contamination is often substantially reversible, though metal ions in the membrane accelerate its decomposition by catalyzing radical formation reactions.

2.2.1. Mitigation strategies

High voltage (especially OCV), low humidity and high temperature are known to accelerate chemical degradation of the membrane. Also, increased operating pressures facilitate radical formation due to increased reactants' crossover. Uneven water humidity distribution along the channel length (e.g. local drying at the inlet) can result in the membrane mechanical strain. Humidity and temperature cycling can cause membrane fatigue.

Some general guidelines could include:

- Operate the cell with high RH and avoid RH cycling
- Operate the cell at moderate temperatures. Trade-off. Avoid temperature cycling.
- Lower operating pressures on the anode. Trade-off.
- Avoid staying at the OCV.
- Prevent freezing conditions within the cell during off periods. Possible solution is warming the cell with additional device (e.g. battery) during off periods to keep the cell temperatures above certain value. Another solution might be effective dry gas purging before shutdown (also helpful to prevent catalyst degradation).

2.3. Gas diffusion layers

Most of the papers on GDLs deal with the influence of GDL materials and design on the fuel cell performance. There are very few papers dealing with GDL degradation and majority of them are done *ex-situ*. One of the main functions of the GDL is to provide passages for the reactant gas diffusion from the channel to the CL. To ensure that, the GDL needs to be able to dispose of the excess water from the CL and GDL to prevent flooding. Hence, GDL degradation is usually associated with an increase in mass transport losses. Excess water (flooding) in GDL or CL obstructs reactant gases in their way to the catalyst site. If the cause of the flooding is just due to temporary non-optimal operating conditions, it is often substantially reversible simply by adjusting them (often just raising the cell temperature). But, if the flooding is caused by the irreversible structural changes in the GDL, mitigation technics may prove futile. There are three major causes of the GDL degradation: 1) carbon corrosion [18], 2) PTFE decomposition [19] and 3) mechanical degradation as a result of compression [20]. The first two mechanisms cause hydrophobicity loss and changes in the GDL pores structure. Carbon particles and carbon fibers in the GDL are more stable than the carbon particles in the CL, due to absence of Pt, but are still prone to corrosion. It was shown that at high voltages (>1.2 V) carbon corrosion led to thinning of the GDL fibers, which resulted in increased ohmic, charge and transfer resistance [21]. Experiments have also shown an increase in micro porous layer (MPL) pore sizes due to the loss of the carbon particles in the MPL. Carbon fibers are usually treated with PTFE to protect them, but it was shown that the GDL loses its hydrophobicity over time due to PTFE decomposition, though this phenomenon is not clearly understood [19]. Importantly, operation under flooding conditions seems to wash out MPL [22].

2.3.1. Mitigation strategies

Mitigation strategies for CL degradation also apply here. This especially applies to startup and shutdown procedures. Also, effective purging to minimize water condensation during off periods should retard hydrophobicity loss.

3. Accelerated stress test protocols

Durability of a fuel cell is most often defined as the maximum lifetime of a fuel cell system with less than 10% loss in efficiency at the end of life [5]. The requirements for minimum fuel cell durability vary significantly, depending on their application. US Department of Energy (DOE) set the targets of 40 000 and 5 000 hours for stationary and transportation applications, respectively [23]. While still significantly short of those targets, fuel cells already exhibit lifetimes in excess of 10 000 and 1700 hours for stationary and transportation applications, respectively [24]. Testing a fuel cell in real life operating conditions would consequently not only take a very long time to conduct a test (40 000 hours means about 4.5 years of uninterrupted testing), but also lead to very high fuel expenses. It is estimated that testing a 275 kW fuel cell bus system for 20 000 hours would

FB – Analysis of Degradation Mechanisms

result in about 2 million US dollars of hydrogen fuel expenses only [5]. Therefore, the fuel cell industry had to come up with accelerated stress protocols (AST) that would significantly reduce the time and resources needed to conduct the tests while at the same time obtaining meaningful results. It is important that test conditions and procedures do not result in decay mechanisms different from those experienced during normal operation. Usually, degradation of a fuel cell can be accelerated by increasing stress level above those experienced in the field, or by increasing its frequency. Stressors and their impact on the fuel cell degradation are listed in

Table 2 [3]. It is interesting to note that low potentials or high loads are not known to accelerate degradation in PEM fuel cells. Hence, most AST protocols consist of either high potential holds (usually OCV or higher; imposed potential) or frequent cycling. Both are often coupled with high temperature as it accelerates all adverse processes.

Table 2 Stressors and decay mechanisms

STRESS		DECAY MODE				
Type	Magnitude	Carbon corrosion	Platinum dissolution	Membrane damage*	Structural damage**	Activity loss***
Potential	High	X	X			
	Low					
	Cycles	X	X	X		
Humidity	High	X	X			
	Low			X		
	Cycles			X		
Load	High					
	Low	X				
	Cycles	X	X	X		
Temperature	High	X	X	X		
	Low (freezing)				X	
	Cycles				X	
Contaminants	High			X		X

    * Mechanical and chemical degradation,
    ** Physical changes, especially to the electrode layers,
    *** Activity losses beyond those due to platinum dissolution

US DOE has published four AST protocols to provide a standard of set test conditions and operating procedures to evaluate new cell component materials and structures [25]. Each of these AST protocols is designed so to specifically target one of four critical decay modes in an MEA: catalyst degradation, catalyst support degradation, membrane chemical degradation and membrane mechanical degradation. Test protocols and metrics are shown in Tables 3-6. The specific conditions of each and cycles are intended to isolate effects and failure modes and are based on assumed, but widely accepted, mechanisms.

FB – Analysis of Degradation Mechanisms

The AST for electrolcatalyst degradation consists of potential cycling between 0.7 and 0.9 V with 30 seconds rest time at each potential. Recommended duration of the test is 30 000 cycles or until the targeted electrode ECSA decreases by 40%, activity loss reaches 60% or performance is reduced by 30 mV at 0.8 A/cm^2. As the metrics polarization curve, catalytic activity and cyclic voltammetry (CV) measurements are conducted according to defined protocols.

The AST for catalyst support degradation consists of imposing and holding the voltage of 1.2 V at the cell's temperature of 95 °C. Recommended duration of the test is 200 hours or until the targeted electrode ECSA decreases by 40%, activity loss reaches 60% or performance is reduced by 30 mV at 1.5 A/cm^2. For metrics on-line CO_2 monitoring is added to standard set of diagnostic tools.

The AST for membrane chemical stability consists of holding the MEA at the OCV with cell temperature of 90 °C and 30% RH of inlet reactants. Recommended duration of the test is 200 hours or until the hydrogen crossover current equivalent reaches 20 mA/cm^2 or OCV drops down by 20%. Release of fluorides should be monitored (measuring the concentration in effluent water at the exhaust) and hydrogen crossover measured every 24 hours.

The AST for membrane mechanical stability consists of cycling the RH of inlet gases from completely dry to over saturated (90 °C dew point at the cell temperature of 80 °C). Each setting should be kept for two minutes (four minutes cycle) and 20 000 cycles should be conducted or until gas crossover reaches 10 sccm according to defined protocol.

Table 3 DOE AST protocol for electrocatalyst

Electrocatalyst Cycle and Metrics		
Cycle	Step change: 30s at 0.7V and 30s at 0.9 V. Single cell 25 - 50cm²	
Number	30,000 cycles	
Cycle time	60 s	
Temperature	80°C	
Relative Humidity	Anode/Cathode 100/100%	
Fuel/Oxidant	Hydrogen/N_2	
Pressure	150 kPa absolute	
Metric	Frequency	Target
Catalytic Activity*	Beginning and End of Life	≤60% loss of initial catalytic activity
Polarization curve from 0 to ≥1.5 A/cm^2**	After 0, 1k, 5k, 10k, and 30k cycles	≤30mV loss at 0.8 A/cm^2
ECSA/Cyclic Voltammetry	After 1, 10, 30, 100, 300, 1000, 3000 cycles and every 5000 cycles thereafter	≤40% loss of initial area
*Activity in A/mg @ 150kPa abs backpressure at 900mV iR-corrected on H_2/O_2, 100%RH, 80°C		
** Polarization curve per USFCC "Single Cell Test Protocol" Section A6		

FB – Analysis of Degradation Mechanisms

Table 4 DOE AST protocol for catalyst support

Catalyst Support Cycle and Metrics		
Cycle	Hold at 1.2 V for 24h; run polarization curve and ECSA; repeat for total 200h. Single cell 25 - 50 cm^2	
Total time	Continuous operation for 200 h	
Diagnostic frequency	24 h	
Temperature	95°C	
Relative Humidity	Anode/Cathode 80/80%	
Fuel/Oxidant	Hydrogen/Nitrogen	
Pressure	150 kPa absolute	
Metric	Frequency	Target
CO$_2$ release	On-line	<10% mass loss
Catalytic Activity*	Every 24 h	≤60% loss of initial catalytic activity
Polarization curve from 0 to ≥1.5 A/cm^2**	Every 24 h	≤30mV loss at 1.5 A/cm^2 or rated power
ECSA/Cyclic Voltammetry	Every 24 h	<40% loss of initial area
*Activity in A/mg @ 150kPa abs backpressure at 900mV iR-corrected on H$_2$/O$_2$, 100%RH, 80°C		
**Polarization curve per USFCC "Single Cell Test Protocol" Section A6		

Table 5 DOE AST protocol for membrane chemical stability

MEA Chemical Stability and Metrics		
Test Condition	Steady state OCV, single cell 25 - 50cm^2	
Total time	200 h	
Temperature	90°C	
Relative Humidity	Anode/Cathode 30/30%	
Fuel/Oxidant	Hydrogen/Air at stoics of 10/10 at 0.2 A/cm^2 equivalent flow	
Pressure, inlet kPa abs (bara)	Anode 250 (2.5), Cathode 200 (2.0)	
Metric	Frequency	Target
F release or equivalent for non-fluorine membranes	At least every 24 h	No target – for monitoring
Hydrogen Crossover (mA/cm^2)*	Every 24 h	≤20 mA/cm^2
OCV	Continuous	≤20% loss in OCV
High-frequency resistance	Every 24 h at 0.2 A/cm^2	No target – for monitoring
*Crossover current per USFCC "Single Cell Test Protocol" Section A3-2, electrochemical hydrogen crossover method		

FB – Analysis of Degradation Mechanisms

Table 6 DOE AST protocol for membrane mechanical stability

Membrane Mechanical Cycle and Metrics (Test using a MEA)		
Cycle	Cycle 0% RH (2 min) to 90°C dewpoint (2 min), single cell 25 - 50cm^2	
Total time	Until crossover >10 sccm or 20,000 cycles	
Temperature	80°C	
Relative Humidity	Cycle from 0% RH (2 min) to 90°C dewpoint (2 min)	
Fuel/Oxidant	Air/Air at 2 slpm on both sides	
Pressure	Ambient or no back-pressure	
Metric	**Frequency**	**Target**
Crossover*	Every 24 h	≤10 sccm
*Crossover per USFCC "Single Cell Test Protocol" Section A3-1, pressure test method with 3 psig N$_2$		

4. Degradation research at FESB

In order to get some practical experience and understanding of underlying degradation mechanisms on a MEA two accelerated stress experiments were conducted at FESB's Laboratory for New Energy Technologies. The laboratory is equipped with the Medusa fuel cell test station Model 890CL with impedance spectroscopy analyzer integrated, Hogen GC 600cc/min hydrogen generator and BioLogic SP-150 potentiostat/galvanostat. High purity hydrogen produced via hydrogen generator, synthetic air and nitrogen are used as a fuel, oxidant and purge gas, respectively.

The first experiment was conducted exactly according to DOE AST protocol for membrane chemical stability. The second one was somewhat modified DOE AST protocol for electrocatalyst degradation. Both experiments were conducted on single cells in a co-flow configuration with 50 cm^2 active area membranes manufactured by BASF (12E-W MEA). In both experiments same diagnostic methods were used to assess the cell's performance. Cell's diagnostics were conducted after certain period of time or number of cycles that the cell was exposed to during the stress test. Cell temperature and backpressures were kept constant in all diagnostic testings, 60 °C and 500 mbarg on both sides, respectively.

Polarization curves were recorded using two steps, 40 mA/cm^2 at lower currents (activation controlled area), and 100 mA/cm^2 at higher currents (ohmic and concentration controlled area). The rest time was set to 20 seconds at each point. Stoichiometry of anode and cathode were 2 and 4 respectively, while the RH was set to 84% for both reactants (dew point of 61 °C).

Tafel slope measurements were recorded with a sweep rate of 2 mV/s between OCV and ≈200 mA/cm^2. The operating conditions were the same as with the polarization curves recordings while the reactants flow rates were set to constant, 0.4 SLPM at the anode and 1 SLPM at the cathode (stoichiometry of 6 at 0.2 A/cm^2).

Electrochemical impedance spectroscopy (EIS) measurements were recorded in the frequency range of 0.1-5012 Hz at the current density 100 mA/cm^2. The operating conditions were the same as with the polarization curves recordings while the reactant flow rates were set to constant, 0.4 SLPM on both sides.

Cycling voltammetry (CV) measurements were recorded with anode as a counter and a reference electrode, and cathode as a working electrode. Constant flows of 0.4 SLPM and 100% RH (dew point 65°C) hydrogen and nitrogen were used on anode and cathode, respectively. Five cycles (between 0.1 and 0.6 V) with a sweep rate of 50 mV/s were conducted with the last one being recorded as representative.

Linear sweep voltammetry (LSV) measurements were conducted with all the parameters same as with the CV and a sweep rate of 5 mV/s between 0.1 and 0.5 V.

4.1. OCV degradation

The first experiment was conducted exactly according to the DOE AST protocol for membrane chemical stability, as specified in Table 5. The cell was held at OCV with cell temperature set at 90°C and inlet reactant humidity set at 30% (dew point 61 °C). The only slight deviation from DOE protocol was that the reactants' flows were set to correspond to a stoichiometry of five at 0.2 A/cm^2 as opposed to DOE recommendation of ten. This was done in order to decrease consumption of gases. Backpressures were held at 500 mbarg on both sides. High voltages accompanied with high temperatures and low RH are known to accelerate membrane chemical decomposition. It is generally accepted that the highly oxidative radicals generated during fuel cell operation degrade PFSA membrane due to their high propensity to extract hydrogen atoms from O-H and C-H bonds in the membrane. Degradation is characterized by thinning end emission of HF, CO_2 and H_2SO_4. As a direct consequence of membrane thinning gases crossover (especially hydrogen) increases, which usually leads to rapid cell failure, Figure 2.
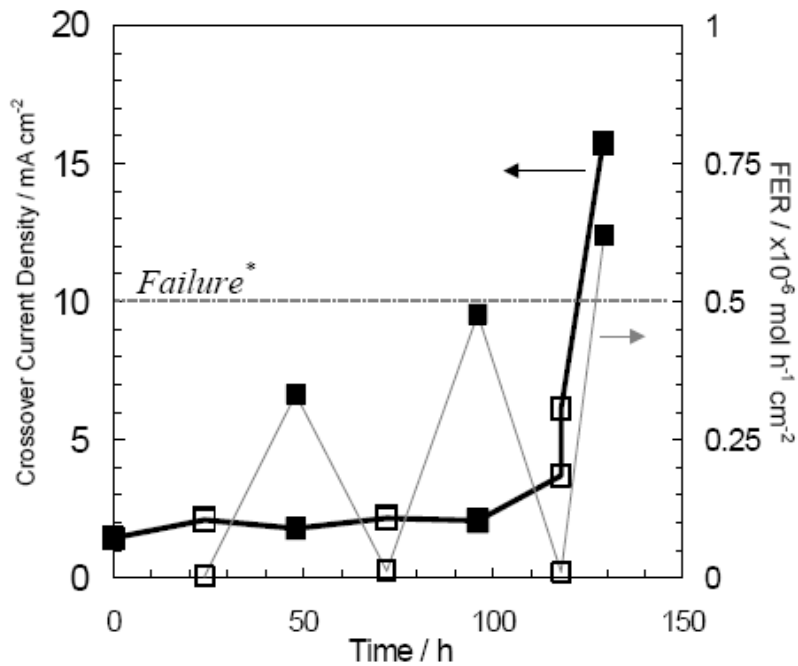
Figure 2 Crossover current density and fluoride emission rate (FER) over time

The fuel cell performance testing (diagnostics) intervals were initially scheduled to every 24 hours. However, since the MEA degraded much faster than expected, last testing was done after only twelve hours after which the experiment was stopped. The experiment was stopped after only 60 hours as it was concluded that the cell's performance deteriorated too much.
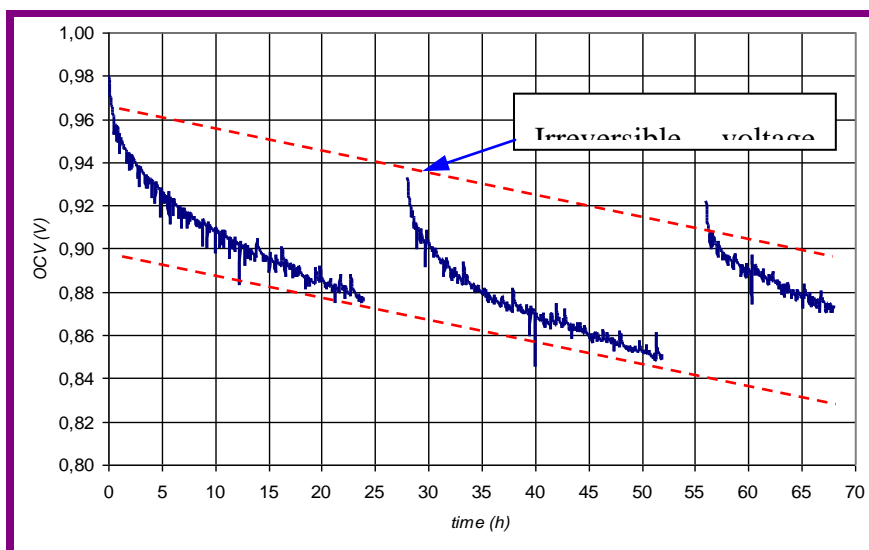

Figure 3 OCV degradation at 90 °C and 30% RH

FB – Analysis of Degradation Mechanisms

In Figure 3 OCV degradation with the time is shown. At the beginning of each OCV degradation procedure, the voltage was relatively high and would afterwards drop gradually with time. After each cycle the OCV would partially recover in comparison with an ending point of the previous cycle. This is in accordance with the other reported OCV degradation research [26][27][28]. This indicates that OCV degradation consists of both reversible and irreversible processes. Reversible voltage loss is believed to be due to adsorption of contaminants or platinum oxidation. Contaminants may be either harmful species generated on the catalyst surface as a result of H_2 and O_2 interaction, or the membrane decomposition products [27][29]. Sugawara et al [29] concluded that the sulfates (SO_4^{2-}) resulting from membrane decomposition adsorb on the catalyst surface. Experiment interruptions for diagnostic reasons would result in the OCV recovery. Diagnostics techniques involve operation at high loads/low potential, high RH, and the flushing of the cathode compartment with nitrogen (CV testing), which all are believed to be beneficial for cleaning the CL, and thus degradation recovery. Voltage recovery after the second interruption (at 56 hours) was even higher than after the first one due to an additional recovery technique applied, consisting of voltage cycling, which will be explained in detail shortly.

In Figure 4 influence of OCV degradation on polarization curve is shown. The polarization curve at the BOL (0 hours) was recorded after break-in. Before recordings of the subsequent curves, the cell parameters were changed from the ones for the AST to the ones for polarization curve recordings. Namely, cell temperature would be decreased to 65 °C and reactant's flow was switched to stoichiometric. The fuel cell would then be left running for 30 min at the 0.2 A/cm^2 prior to recording. Similar procedures, in order to equilibrate the MEA with the new operating conditions and to reach steady state conditions, were conducted before other measurements, as well.
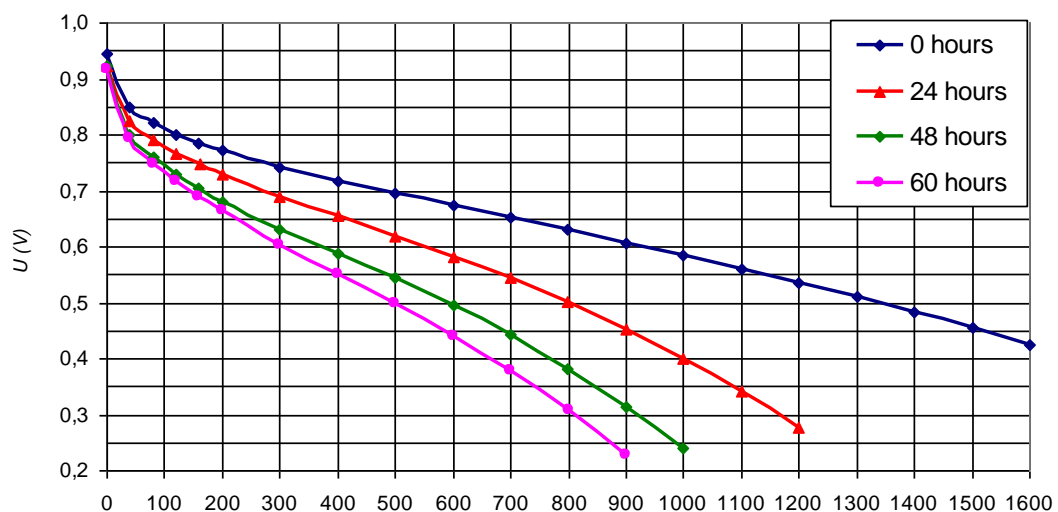

Figure 4 OCV degradation influence on polarization curve

Rapid decrease in performance was noticed even after only 24 hours. After 48 and 60 hours of AST, recovery procedure consisting of potential cycling between 0.6 and 0.9 V with the 30 seconds rest time at each value was conducted. The recovery procedure lasted for about 40 minutes. In Figure 5 fuel cell performance before and after recovery procedure is shown. The

FB – Analysis of Degradation Mechanisms

cell performance improved a lot, but curiously, improvement was only significant at higher current densities. No significant change in ohmic resistance was noticed after recovery procedure, though. The recovery procedure parameters were chosen arbitrarily but similar to the ones proposed in [27]. Authors in [29] propose flooding the cell as a recovery technique, by either supersaturating the inlet flow or decreasing the cell temperature, in order to wash out the anions adsorbed on the catalyst.
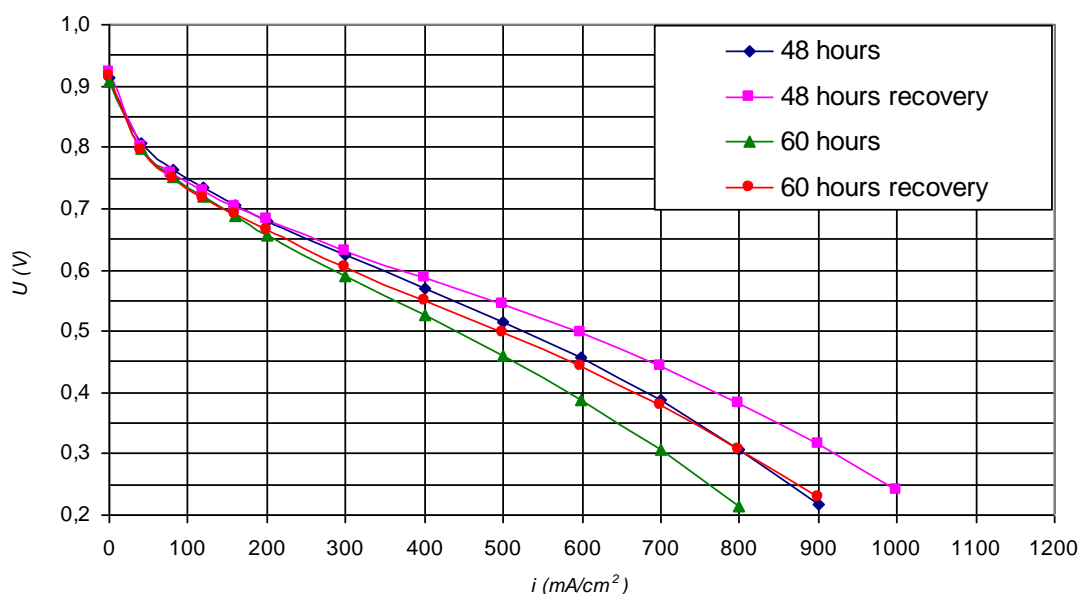

Figure 5 Polarization curve improvements after recovery procedure

In Figure 6 ohmic resistance and EIS at 100 mA/cm^2 are presented. Ohmic resistance increased from initial values of ≈110 mOhm*cm^2 to final values of ≈150 mOhm*cm^2 with the biggest increase in the initial stages. This loss is probably because of the increased contact resistance due to catalyst agglomeration and carbon corrosion in the CL and because of delamination of layers. Nyquist plot of EIS also reveals increase of the total resistance in the activation controlled area. The small semicircle at low frequencies, associated with mass transport losses, increases and completely merges with the big semicircle at 48 hours.

In Figure 7 CV and LSV measurements are given. It can be seen that the ECSA drop down almost 40% after only 24 hours and 65% after 48 hours, only to recover slightly after 60 hours (60% loss). However, it should be noted that the CVs at 48 and 60 hours were taken before their respective recovery procedures. Astonishingly, recovery procedure conducted at 48 hours resulted in higher ECSA even after twelve hours of additional OCV degradation (ECSA at 60 hours higher than at 48 hours). LSV measurements show no detectable change in hydrogen crossover with values being around 1.9 mA/cm^2 throughout the whole experiment. It may seem surprising that despite being exposed to very harsh conditions, membrane did not exhibit increased hydrogen crossover with time. It was shown that OCV degradation causes largely uniform degradation and therefore uniform thinning of membrane across the active area [14]. During the experiment effluent water from the cell exhaust was collected for fluoride emission analysis. Due to technical difficulties, only

FB – Analysis of Degradation Mechanisms

cathode exhaust for the periods of 0-24 and 48-60 hours was analyzed and a slight increase in the fluoride concentration was noticed, 0.496 vs 0.459 mg F⁻/l.
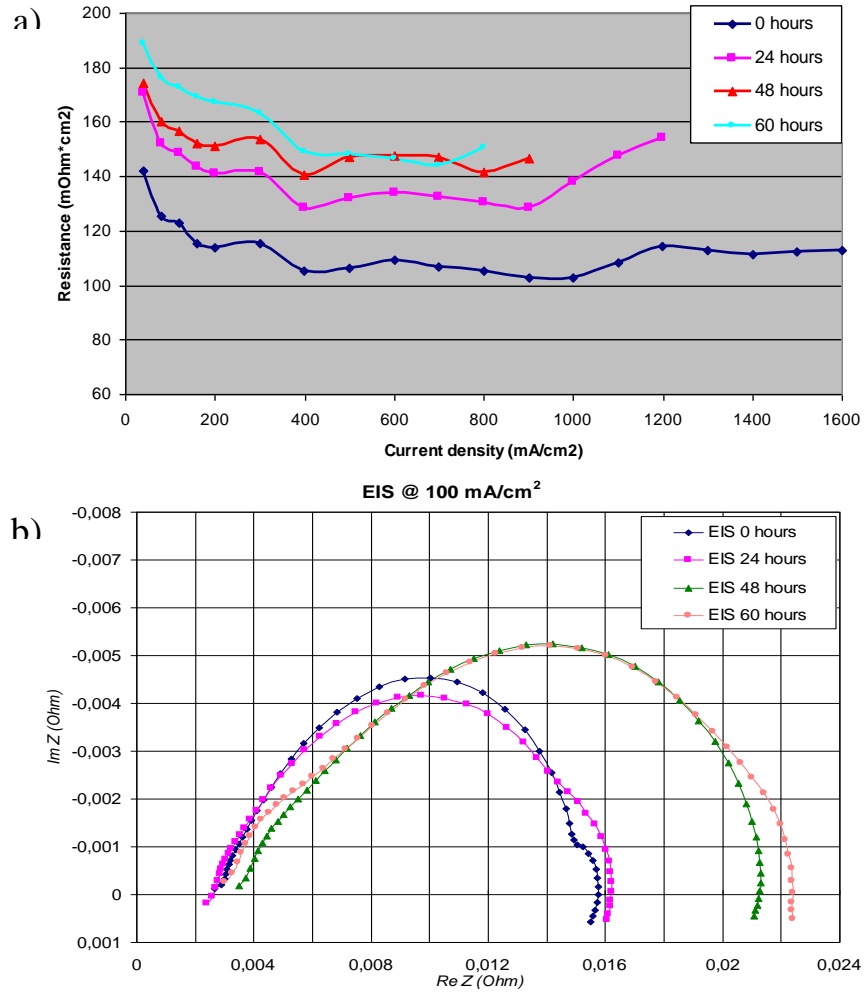

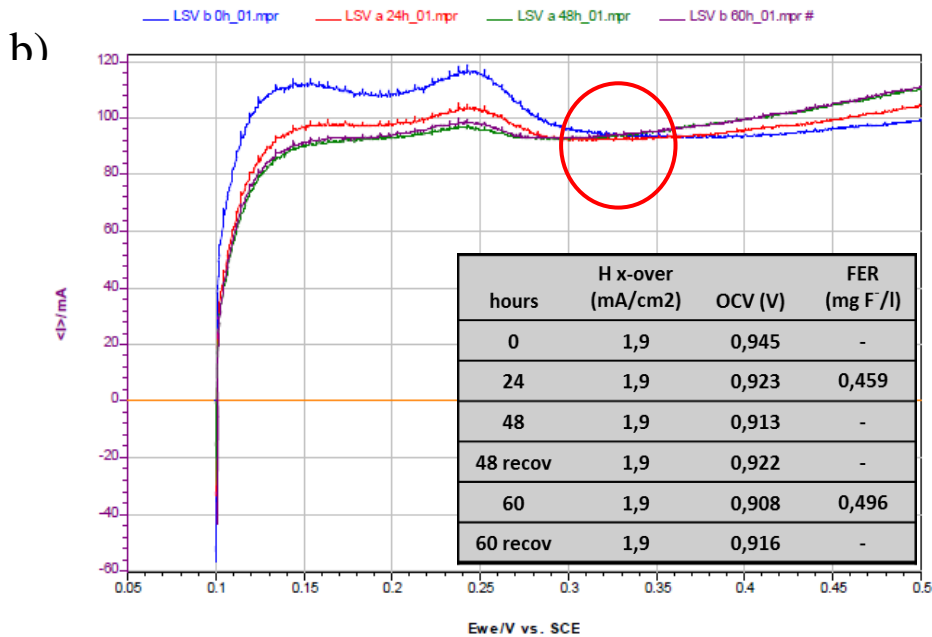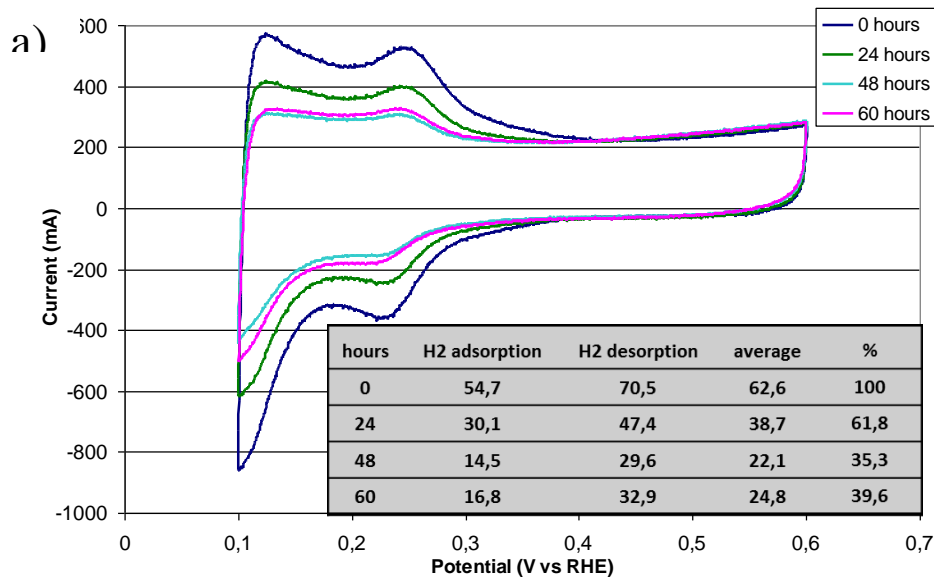**Figure 6** a) Ohmic resistance, b) EIS at 100 mA/cm^2

Figure 7 a) CV and b) LSV measurements for the OCV degradation

Tafel slope measurements are used to evaluate catalytic activity of the fuel cell catalyst. They are usually recorded with high sweep rates at low current densities and high stoichiometries to exclude the contribution of mass transport. With voltage readings corrected for the ohmic voltage drop (iR-corrected) and plotted in a logarithmic scale, the obtained curve should ideally result in a straight line with a slope equal to the Tafel coefficient, *b*. Additionally, the curve is usually corrected for hydrogen crossover by simply shifting the whole curve to the right for the value of hydrogen crossover equivalent current density.

FB – Analysis of Degradation Mechanisms

In Figure 8 Tafel plots in a logarithmic scale are shown. It can be seen that the curves shift down with time while as well as that the slopes appear to increase. Also, the point where the curve deviates from linearity, which should indicate the appearance of mass transport, shifts to the left with time. Linear regression analysis was used to obtain the best logarithmic fit for each curve with $R^2>0.999$ in all cases. Also, no less than twelve point readings for each curve were used for the analysis. Two different approaches were used for the logarithmic fit. In the first one, logarithmic functions were fitted against the readings in the same current density range of 15-50 mA/cm^2 for all the curves. In the second approach, logarithmic functions were fitted against the readings in the same voltage range of 0.85-0.9 V for all the curves. The domains for both fitting approaches are shown in Figure 10. It is well known that the state of Pt surface oxidation influences oxygen reduction reaction (ORR) and ultimately the Tafel slope itself. It is postulated that the Tafel slope of ≈60-70 mV/dec corresponds to a potential regime where oxygen reduction proceeds on a Pt-oxide covered surface (Temkin conditions), while the slope of ≈120 mV/dec is associated with Langmuirian kinetics on oxide-free Pt surface. Oxidized Pt surface is associated with high cathode potentials, ≈0.9 V, while at voltages ≈0.6 V Pt surface is believed to be completely oxide-free. Since with the MEA degradation the same current range falls into an ever decreasing voltage range, Tafel slopes were compared for both same current and voltage ranges.
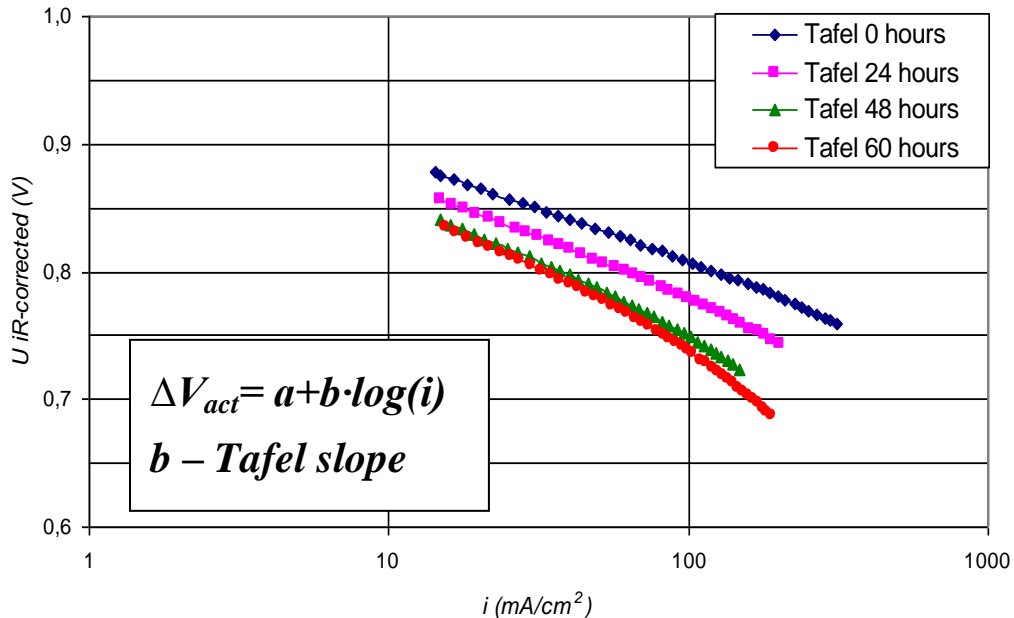

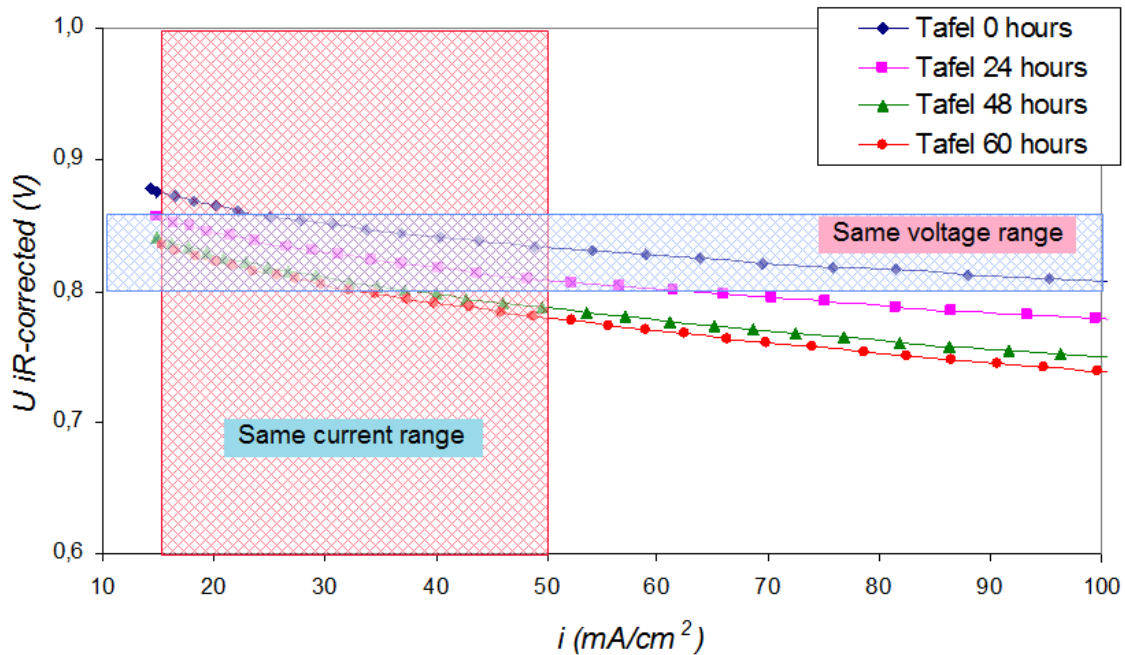**Figure 9** Tafel slopes evolution for the OCV degradation

Figure 10 Different logarithmic fit ranges to obtain a Tafel slope coefficient

In **Tafel slope** increase with degradation, on the other hand, can be caused by the so-called "double tafel slope". The double Tafel slope can develop for highly degraded MEAs where mass transport within the CL starts taking part at low current densities. There are two cases: a) oxygen transport and b) proton transport (ohmic losses) [7]. At this stage, it is too early to make a final judgment on this and further tests are needed in order to elucidate the Tafel slope increase.

Table 7 obtained Tafel slopes for both approaches are given. There is almost no difference between obtained values in both approaches. It should be noted here though, that it takes some time for the Pt surface to oxidize and deoxidize, hence if sweeps are conducted fast enough, there should be no difference. However, the values obtained are somewhat higher than those reported in the literature and what is more, they increased with the MEA degradation. While majority of the authors in the literature report their Tafel slopes to be around theoretical 60-70 mV/dec, our initial values are in the 80-90 mV/dec range. Since all our fits were almost perfect, with $R^2>0.999$, and the results were repeated on a number of tests, we have no reason doubt them. Kabasawa et al [32] also reported similar values for Nafion membrane (80-100 mV/dec) depending on the cathode RH, but they did not change with the degradation, though their degradation levels were not as excessive as in our case.

Tafel slope increase with degradation, on the other hand, can be caused by the so-called "double tafel slope". The double Tafel slope can develop for highly degraded MEAs where mass transport within the CL starts taking part at low current densities. There are two cases:

a) oxygen transport and b) proton transport (ohmic losses) [7]. At this stage, it is too early to make a final judgment on this and further tests are needed in order to elucidate the Tafel slope increase.

Table 7 Tafel slope coefficients for different ranges for the OCV degradation

hours	b (mV/dec) 15-50 mA/cm2	b (mV/dec) 0,85 – 0,8 V
0	86	88
24	96	96
48	109	109
60	113	113

4.2.   Potential cycling degradation

The second experiment was done with the aim to degrade the Pt catalyst by potential cycling. Potential cycling is a known stressor for catalyst degradation. At high cathode potential (≈0.9 V) the Pt catalyst surface is partially oxidized, and the Pt-oxide layer forms a protective shield that slows down Pt dissolution. The idea of potential cycling is that by shortly lowering the cathode potential, the Pt surface gets deoxidized and thus the protective oxide layer is reduced (or completely removed), making the Pt catalyst more vulnerable to subsequent excursion to higher potentials. In the conducted experiment, the general guidelines of the DOE AST protocol for electrocatalyst degradation were followed with several modifications. This protocol suggests cycling between 0.9 and 0.7 V with 30 seconds rest time at each limit, Table 3. Uchimura et al [33][34] showed that catalyst degradation is a function of potential span, rest times and cycle profile. It was shown that catalyst degradation increases with wider potential span, with the highest degradation rate being for the entire span of oxide-free and oxide-covered regimes. They have also shown that it takes around 30 seconds for Pt-oxide layer to form at higher voltages (0.95 V in their case), while as little as ≈3 seconds is enough for the Pt surface to get deoxidized at 0.6 V. In the wake of these findings and in order to speed-up the degradation process and thus saving on both the time and the fuel consumed, we have decided to modify potential profile recommended by DOE. The lower potential limit was set to be 0.6 V with the rest time of 10

FB – Analysis of Degradation Mechanisms

s as opposed to the DOE recommendation of 0.7 V and 30 s rest time. Upper potential and the respective rest time were kept the same as in the DOE AST (0.9 V and 30 s). Due to equipment limitations, fast sweep ramps were employed between the potential limits, 50 mV/s in the ascending, and 100 mV/s in the descending direction. This actually retards the degradation slightly as the catalyst degradation increases with higher anodic (ascending) ramps, with the highest one being for the square cycle (instantaneous jump) [34]. The total cycle duration was 49 seconds, eleven seconds shorter than for the DOE AST. The complete cycle profile is pictured in Figure 10.
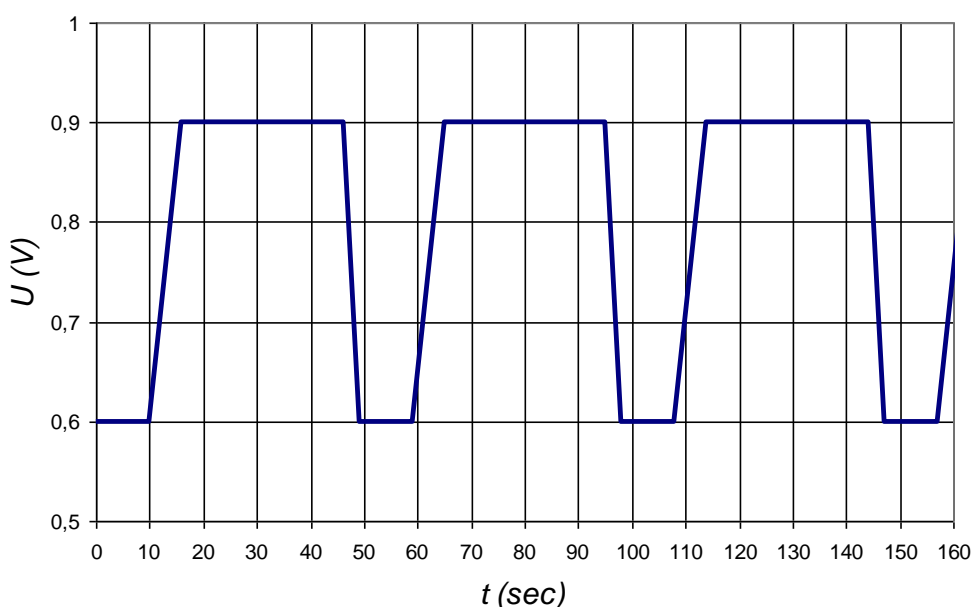

Figure 11 Cycle profile for potential cycling stress test

All the other parameters were kept the same as in the DOE protocol: cell temperature was at 80 °C, the RH of both gases was 100% and nitrogen was used on the cathode side. Using nitrogen on the cathode side means that the cell is in a "driven mode", i.e. voltage is imposed via an external device. Studies have shown that there is no detectable difference in the catalyst degradation between operation with air and nitrogen at 100% RH [33][4]. Apparently, oxygen from the reactant gases does not play a critical role in the oxide coverage [35]. Even though using air is more realistic, using nitrogen on the cathode offers several advantages. Firstly, it helps isolating only catalyst degradation by excluding other possible degradations caused by operating regime: thermal stresses associated with high load changes between high and low voltages, flooding and possible gas starvation due to sudden changes of load. Secondly, it is more economical as for example, gases consumption at 0.6 V can be very high. And thirdly, it is difficult to control the iR corrected voltage that the catalyst actually experiences, and that in turn causes catalyst degradation, in an operating cell (with an oxidant on the cathode).

In Figure 11 potential cycling influence on polarization curve, ohmic resistance and EIS is presented. The experiment was stopped after 5000 cycles (about 68 hours) as it was concluded that the cell's performance deteriorated too much. This is much less than it is

FB – Analysis of Degradation Mechanisms

required by the DOE standards and it was once again proven that the old batch BASF MEAs are not very resilient. As in the previous experiment, after each degradation interval and prior to conducting diagnostic measurements, the cell would be preconditioned for a certain period of time to equilibrate the MEA with the new operating conditions and to reach steady state.
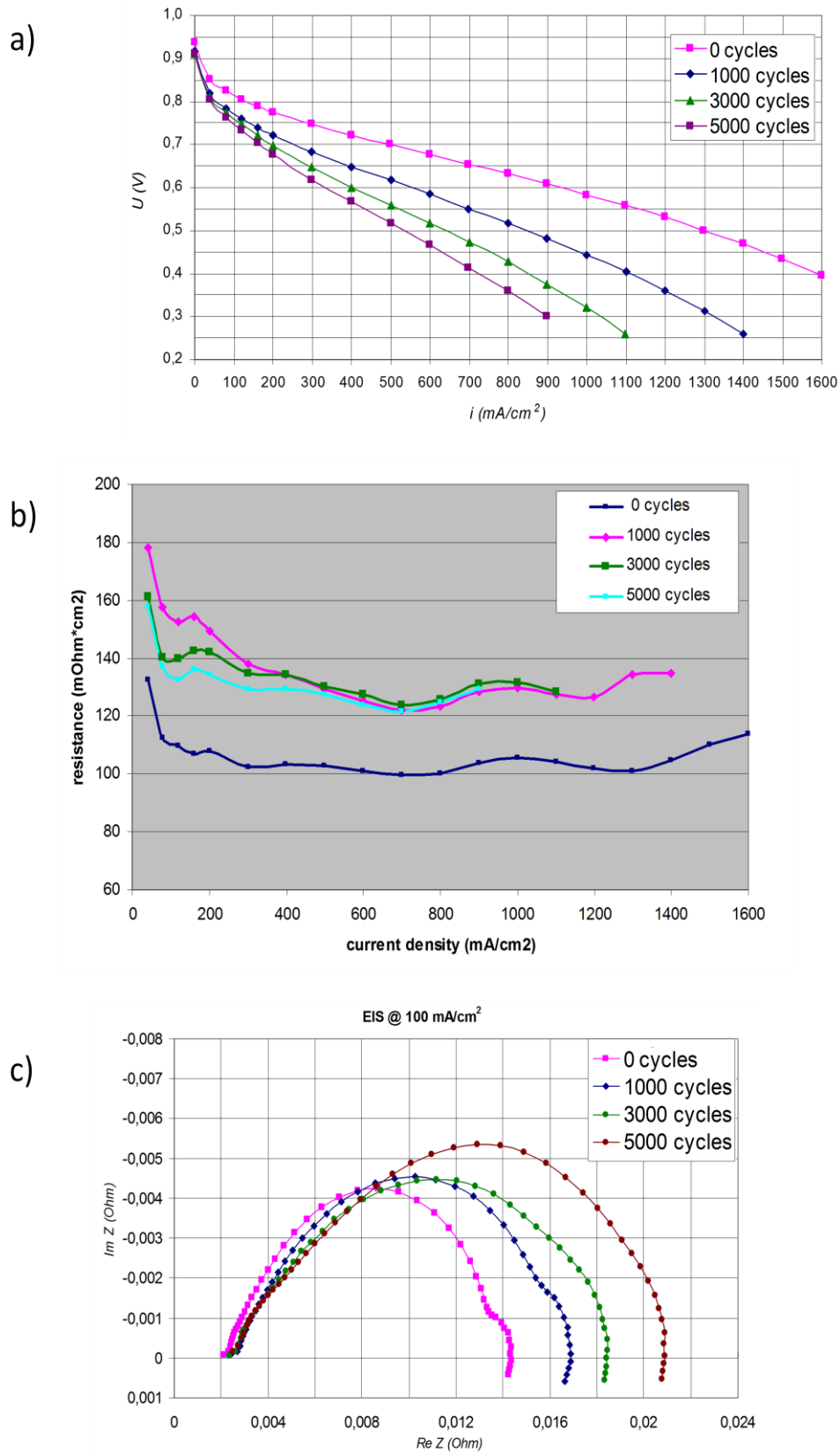
Figure 12 Potential cycling influence on a) polarization curve, b) ohmic resistance and c) EIS at 100 mA/cm2

FB – Analysis of Degradation Mechanisms

Overall, the MEA degradation was a little lower than in the first experiment as the curve after 5000 cycles (≈68 hours) performed better than the curve after 60 hours in the first experiment. From the polarization curves it is obvious that the kinetic performance decreases fast, but there is no characteristic mass transport drop at high current densities associated with problems in gas diffusion. It can be also confirmed in the Nyquist diagram as the semicircle at low frequencies seems to grow slower than in the previous experiment. Ohmic resistance rose around 20% in the first 1000 cycles, but then kept stable for the remaining 4000 cycles.

Table 8 shows that the Tafel slope coefficient again increases with the degradation, though this time this increase has been somewhat lower.

Table 8 Tafel slope coefficients for different ranges for the potential cycling degradation

cycles	b (mV/dec) 15-50 mA/cm2	b (mV/dec) 0,85 – 0,8 V
0	84	96
1000	92	93
3000	103	103
5000	104	104

And finally, in Figure 13, voltammograms and relative change of ECSA over time are shown. ECSA degraded much faster than in the first experiment, and this degradation followed a regressive rate. LSV measurements were also monitored; the hydrogen crossover expectedly did not change and it was around 2 mA/cm^2, just like in the first experiment.
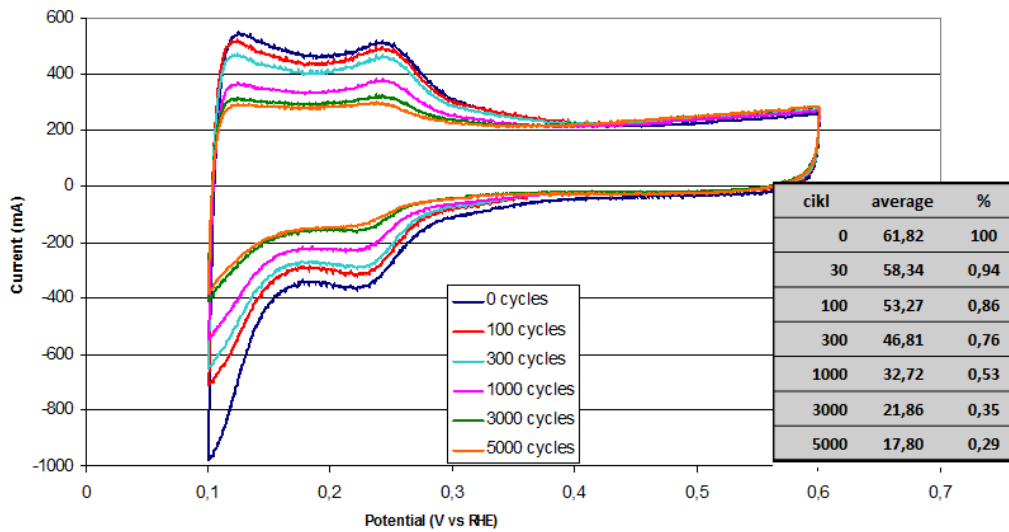
FB – Analysis of Degradation Mechanisms

Figure 13 CV measurements for the potential cycling degradation

cikl	average	%
0	61,82	100
30	58,34	0,94
100	53,27	0,86
300	46,81	0,76
1000	32,72	0,53
3000	21,86	0,35
5000	17,80	0,29

5. Conclusions and future work

One of the main goals of the experiments was to get the first-hand experience on the fuel cell degradation phenomena. Two different stress tests were applied with different goals. It was concluded that both long open circuit voltage (OCV) exposures and high span voltage cycling damage the membrane-electrode assembly (MEA) tremendously. Whereas in the first case significant membrane decomposition took place, no hydrogen crossover was detected. At the same time OCV decay was caused by both reversible and irreversible degradation. Reversible decay is recoverable by simple potential cycling, though it is detrimental to catalyst layer (CL), or by flooding the channels to wash out the contaminants (not done in the experiment). Irreversible OCV decay was associated with the loss of electrochemical surface area (ECSA) and therefore decrease of apparent exchange current density. Therefore, using an OCV loss as an indicator for an increased crossover and thus membrane chemical degradation may be misleading. High irreversible loss of the ECSA is associated with Pt degradation (dissolution and agglomeration) helped by the probable corrosion of carbon support. Potential cycling stress test caused rapid ECSA loss. Still the performance was less influenced than with the OCV degradation. Polarization curve of the MEA after 5000 potential cycles (≈68 hours) was better (especially at higher currents) than the polarization curve of the MEA after 60 hours of OCV degradation, even though the ECSA loss was higher for the former (71% vs 60% loss). This is a further indication that the mass transport losses were higher in the first experiment, most probably due to higher corrosion of the carbon support. One thing that will surely need further examination is Tafel slope measurements. Normally, Tafel slopes should not change with the time. This means that the rate determining step and transfer coefficient for the ORR should remain more or less the same. The unexpected rise in the Tafel slope during degradation can point to a "double Tafel slope", which can happen in highly degraded fuel cell where mass transport within the CL becomes a problem at even small current densities. If this is the case, then the higher rise of

FB – Analysis of Degradation Mechanisms

the Tafel slope in the first experiment would be yet another indication of higher carbon corrosion than in the second experiment. Understanding and interpretation of the Tafel slope is one of the future tasks.

Ideally, one would like to develop a diagnostic procedure to quickly asses the state of the health of an operating fuel cell. The idea would be to plot polarization-change curves over time and monitor the changes in different types of polarization. Critical role in this would be making a quick and precise estimation of the cell's activation polarization contribution. Since Tafel slope gives a good insight into this, defining an exact procedure of conducting its measurement and being able to interpret the result is of paramount importance. Sweep rate and range have to be defined, and also it appears from the preliminary tests that the operating point of the cell prior to the execution of the Tafel sweep plays a role. Determining the point of the slope deviation from linearity would help assessing mass transport evolution over time. Also, in case of "double Tafel slope" one has to be able to determine if the problem is with oxygen transport or ionic losses within the CL.

Most likely degradation stressors that may be expected in a fuel cell used in combined heat and power (CHP) applications are fuel starvation, temperature excursions above the normal operating temperature, and resulting drying or flooding that may happen during transients, i.e., changing the power level, as well as contamination coming from the fuel processor which may also happen during transients but also during normal steady state operation. The work during the next reporting period will be devoted to exploration of these stressors, and detection, identification and quantification of their symptoms. Stress tests with more realistic operating conditions and load profiles will be performed, namely with load profiles that the fuel cell would be expected to experience in CHP applications. Predefined quick diagnostic procedures would be executed after certain periods with the goal of making a quick assessment of the cell's state of health by comparing the polarization-change curves. Before conducting tests with the short stack received from ZSW, some of the stressor tests described in this report will be repeated with the same 50 cm^2 single cell but with the MEAs of the same type as in the short stack, in order to find out whether the findings described in this report can be applicable to the short stack.

FB – Analysis of Degradation Mechanisms

References

[1] F. Barbir, PEM Fuel Cells: Theory and Practice, 2nd Edition, Elsevier Academic Press, 2012

[2] M. Perry, R. Balliet and R. Darling, Experimental Diagnostics and Durability Testing Protocols, in "Modern Topics in Polymer Electrolyte Fuel Cell Degradation", M. Mench, E. Kumbur and T. Veziroglu, Editors; Elsevier, 2011 pp. 335-362

[3] M. Perry, Durability of Polymer Electrolyte Fuel Cells, in "PEM Fuel l Cells: Theory and Practice, 2nd Edition", Elsevier Academic Press, 2012

[4] S. Kocha, Electrochemical Degradation: Electrocatalyst and Support Durability, in "Modern Topics in Polymer Electrolyte Fuel Cell Degradation", M. Mench, E. Kumbur and T. Veziroglu, Editors; Elsevier, 2011 pp. 89-214

[5] Jianlu Zhang, H. Zhang, J. Wu, Jiujun Zhang, PEM Fuel Cell Testing and Diagnosis, Elsevier, 2013

[6] S. Strahl, A. Husar, A. Franco, Electrode Structure Effects on the Performance of Electrode Structure Effects on the Performance of Open-Cathode Proton Exchange Membrane Fuel Cells: A Multiscale Modeling Approach, Journal of Hydrogen Energy, under review

[7] K. O'Neil, J. Meyers, R. Darling, M. Perry, Oxygen gain analysis for proton exchange membrane fuel cells, Journal of Hydrogen Energy, 37 (2012) 373-382

[8] C.A. Reiser, D.Yang, R.D. Sawyer, Procedure for shutting down a fuel cell system using air purge US6858336, 2005

[9] S.S. Kocha Mitigating fuel cell start up/shut down degradation US20060240293 2005

[10] C. Gittleman, F. Coms and Y. Lai, Membrane Durability and Chemical Degradation, in "Modern Topics in Polymer Electrolyte Fuel Cell Degradation", M. Mench, E. Kumbur and T. Veziroglu, Editors; Elsevier, 2011 pp. 15-88

[11] A. Ohma, S. Suga, S. Yamamoto, K. Shinohara, Membrane Degradation Behavior during Open-Circuit Voltage Hold Test, Journal of Electrochemical Society 2007, 154, B757-60

[12] T. Madden, D. Weiss, N. Cipollini, D. Condit, M. Gummalla, S. Burlatsky, V. Atrazhev, Degradation of Polymer-Electrolyte Membranes in Fuel Cells, J. Electrochem. Soc. 156 (2009) B657–B662.

[13] D. Curtin, R. Lousenberg, T. Henry, P. Tangeman, M. Tisack, Advanced Materials for Improved PEMFC Performance and Life, Journal of Power Sources 131 (1–2) (2004) 41–48

[14] W. Liu, M. Crum, Effective Testing Matrix for Studying Membrane Durability in PEM Fuel Cells: Part I. Chemical Durability, ECS Trans. 3 (1) (2006) 531–540.

[15] E. Holby, W. Sheng, Y. Shao-Horn, D. Morgan, Pt nanoparticle stability in PEM fuel cells: influence of particle size distribution and crossover hydrogen, Energy Environ. Sci. 2 (2009) 865–871.

[16] Y. Fu, A. Manthiram, M. Guiver, Blend Membranes Based on Sulfonated Polyetheretherketone and Polysulfone Bearing Benzimidazole Side Groups for Fuel Cells, Electrochem, Commun 8 (2006) 1386–1390.

[17] C. Gibon, S. Norvez, S. Tence´-Girault, J.T. Goldbach, Control of Morphology and Crystallization in Polyelectrolyte/Polymer Blends, Macromolecules 41 (2008) 5744–5752

[18] M. Cai, M. Ruthkosky, B. Merzougui, S. Swathirajan, M. Balogh, S.Oh, Investigation of thermal and electrochemical degradation of fuel cell catalysts, Journal of Power Sources, (2006) 160 977-86.

[19] M. Schulze, N. Wagner, T. Kaz, K. Friedrich, Combined electrochemical and surface analysis investigation of degradation processes in polymer electrolyte membrane fuel cells, Electrochimica Acta, (2007) 52 2328-36.

[20] C. Lee, W. Merida, Gas diffusion layer durability under steady-state and freezing conditions, Journal of Power Sources, (2007) 164 141-53.

[21] G. Chen, H. Zhang, H. Ma, H. Zhang, Electrochemical durability of gas diffusion layer under simulated proton exchange membrane fuel cell conditions, International Journal of Hydrogen Energy 34 (19) (2009) 8185–8192.

[22] J.-H. Lin, W.-H. Chen, S.-H. Su, Y.-J. Su, T.-H. Ko, Washing Experiment of the Gas Diffusion Layer in a Proton-Exchange Membrane Fuel Cell, Energy & Fuels 22 (4) (2008) 2533–2538.

[23] E. Wargo, C. Dennison and E. Kumbur, Durability of Polymer Electrolyte Fuel Cells: Status and Targets, in "Modern Topics in Polymer Electrolyte Fuel Cell Degradation", M. Mench, E. Kumbur and T. Veziroglu, Editors; Elsevier, 2011 pp. 1-14

[24] Y. Yuan, H. Li, S. Zhang, J. Martin, H. Wang, A review of polymer electrolyte fuel cell durability test protocols, Journal of Power Sources, 196 (2011) 9107-9116

[25] N. Garland, T. Benjamin and J. Kopasz, DOE Fuel Cell Program: Durability Technical Targets and Testing Protocols, ECS Transactions, 11 (1) 923-931 (2007)

[26] S. Kundu, M. Fowler, L. Simon, R. Abouatallah, Reversible and irreversible degradation in fuel cells during Open Circuit Voltage durability testing, Journal of Power Sources, 182 (2008) 254-258.

[27] S. Zhang, X. Yuan, J.Cheng Hin, H. Wang, J. Wu, K. Friedrich, M. Schulze, Effects of open-circuit operation on membrane and catalyst layer degradation in proton exchange membrane fuel cells, Journal of Power Sources 195 (2010) 1142-1148.

[28] S. Zhang, X. Yuan, R. Hiesgen, K. Friedrich, H. Wang, M. Schulze, A. Haug, H. Li, Effect of open circuit voltage on degradation of a short proton exchange membrane fuel cell stack with bilayer membrane configurations, Journal of Power Sources 205 (2012) 290-300

FB – Analysis of Degradation Mechanisms

[29] S. Sugawara, T. Maruyama, Y. Nagahara, S. Kocha, K. Shinohra, K. Tsujita, S. Mitsushima, K. Ota, Performance decay of proton-exchange membrane fuel cells under open circuit conditions induced by membrane decomposition, Journal of Power Sources 187 (2009) 324-331

[30] A. Parthasarathy, C. Martin, Investigation of the O_2 reduction reaction at the platinum/Nafion® interface using a solid-state electrochemical cell, Journal of Electrochemical society, Vol. 138, No. 4 April 1991.

[31] A. Parthasarathy, S. Srinivasan, J. Appleby, Temperature dependence of the electrode kinetics of oxygen reduction at the platinum/Nafion® interface – a microelectrode investigation, Journal of Electrochemical society, Vol. 139, No. 9 September 1992.

[32] A. Kabasawa, J. Saito, K. Miyatake, H. Uchida, M. Watanabe, Effects of the decomposition of sulfonated polyimide and Nafion membranes on the degradation and recovery of electrode performance in PEFCs, Electrochimica Acta, 54 (2009) 2754-2760.

[33] M. Uchimura, S. Kocha, The impact of cycle profile on PEMFC durability, ECS Transactions, 11 (1) 1215-1226 (2007)

[34] M. Uchimura, S. Sugawara, Y. Suzuki, J. Zhang, S. Kocha, Electrocatalyst durability under simulated automotive drive cycles, ECS Transactions, 16 (2) 225-234 (2008)

[35] S. Sugawara, K. Tsujita, S. Kocha, K. Shinohara, S. Mitsushima, K. Ota, Simultaneous electrochemical measurements of ORR kinetics and Pt oxide formation/reduction, 214th Electrochemical Society Meeting, Honolulu, HI, Wednesday, October 16, 2008